Peer-reviewed version available at *Nanomaterials* **2017**, *7*, , 146; doi:10.3390/nano7060146

Article

Highly Sensitive Magnetic-SERS Dual-Function Silica Nanoprobes for Effective On-Site Organic Chemical Detection

Cheolhwan Jeong,[1,†] Hyung-Mo Kim,[2,†] So Yeon Park,[1] Myeong Geun Cha,[3] San Kyeong,[1] Xuan-Hung Pham,[2] Eunil Hahm,[2] Yuna Ha,[2] Dae Hong Jeong,[3] Bong-Hyun Jun[2,*] and Yoon-Sik Lee[1,*]

[1] School of Chemical and Biological Engineering, Seoul National University Seoul 151-742, Republic of Korea; purebeam@naver.com (C.J.); sypark1231@naver.com (S. Y. P.); san.volcano@gmail.com (S.K.);

[2] Department of Bioscience and Biotechnology, Konkuk University, Seoul 143-701, Republic of Korea; hmkim0109@konkuk.ac.kr (H.-M.K.); pahmricky@gmail.com (X.-H.P.); greenice@konkuk.ac.kr (E.H.); wes0510@konkuk.ac.kr (Y.H.);

[3] Department of Chemistry Education, Seoul National University, Seoul 151-742, Republic of Korea; cha6614@snu.ac.kr (M. G. C.); jeongdh@snu.ac.kr (D. H. J.)

* Correspondence: bjun@konkuk.ac.kr (B.-H.J.); yslee@snu.ac.kr (Y.-S.L); Tel.: +82-2-450-0521 (B.-H.J.); Tel.: +82-2-880-7073 (Y.-S.L.)

† These authors contribute equally to this work.

Abstract: We report magnetic silver nanoshells (M AgNSs) that have both magnetic and SERS properties for SERS-based detection. The M AgNSs are composed of hundreds of Fe_3O_4 nanoparticles for rapid accumulation and bumpy silver shell for sensitive SERS detection by near-infrared laser excitation. The intensity of the SERS signal from the M AgNSs was strong enough to provide single particle-level detection. We obtained much stronger SERS signal intensity from the aggregated M AgNSs than from the non-aggregated AgNSs. 4-Fluorothiophenol was detected at concentrations as low as 1 nM, which corresponds to 0.16 ppb. The limit of detection for tetramethylthiuram disulfide was 10 μM, which corresponds to 3 ppm. The M AgNSs can be used to detect trace amounts of organic molecules using a portable Raman system.

Keywords: surface-enhanced Raman scattering; magnetic aggregation; on-site detection

1. Introduction

Surface-enhanced Raman scattering (SERS) has been widely utilized as a powerful tool for molecular analysis because of its narrow bandwidth and stability against photobleaching [1-5]. Each organic molecule has a unique SERS spectrum that can act as a molecular fingerprint; thus, a SERS-active material has been used to identify molecules by SERS signals. In this regard, numerous SERS-active materials have been reported to detect various target chemicals, such as pesticides, polycyclic aromatic hydrocarbons, or food contaminants [6-9]. Among them, novel metal nanoparticles (NPs) are usually exploited for organic chemical detection. The intensity of SERS signal is highly dependent on the plasmonic property of SERS substrates, which can be greatly influenced by the structure of plasmonic NPs. Thus, proper manipulation of the structure of SERS substrates is needed for increased SERS intensity with greater sensitivities for efficient identification of trace contaminants. One of the important factors that characterize SERS-active NPs is the morphology of the NPs [10]. Among various structures, a bumpy shell structure is more desirable than a smooth one for the following reasons: 1) The bumpy shell structure can be excited by a near-infrared (NIR) light source, which can provide valuable advantages, such as fewer disturbances from biomolecules which have auto-fluorescence and a greater tissue penetration capability [11,12]. 2) The NPs can sensitively detect the

targets because the Raman reporter molecules generate much stronger signals when they are located in the gaps between the bumps on the surface [13].

Magnetic properties have been widely utilized as a component of complex nanostructures in multifunctional SERS active NPs [14-17]. They are usually exploited for the separation of cells [18] or small molecules [19] because NP's movement is easily controlled by applying an external magnetic field. Such a special modality could be combined with SERS to acquire a synergetic effect for on-site chemical detection. Magnetic-induced accumulation of SERS active NPs is quite effective for increasing SERS intensity that is closely related with detection sensitivity [20]. In order to obtain the magnetic-SERS dual function NPs which have strong response to an external magnetic field, assembling a large number of magnetic NPs on SERS active NPs rather than using a single magnetic NP is desirable [21]. Although various approaches have been tried to obtain magnetic-SERS dual functionality, some limitations still exist, such as weak magnetization [22,23] or polydispersity of NPs [24].

Herein, we have developed multilayered magnetic-SERS dual-function NPs for ultrasensitive, portable, and on-site Raman-based detection of organic chemicals. The magnetic silver nanoshell (M AgNS) structure was designed to improve the SERS sensitivity. The M AgNSs are composed of hundreds of Fe_3O_4 NPs for rapid accumulation and a bumpy silver shell for sensitive SERS detection using NIR laser excitation, as shown in Fig 1a. Superparamagnetic Fe_3O_4 NPs are immobilized on a silica NP, and covered by an additional silica layer. When an external magnetic field is applied, the M AgNSs show a strong response to the magnetic field because of a large amount of Fe_3O_4 NPs assembled on the nanostructure. A silver shell is formed on the outer layer of the silica-coated Fe_3O_4 NP-embedded silica NP (magnetic silica NP) with a bumpy structure, which leads to an intrinsically strong SERS signal [13]. The dual functionality of the M AgNSs can be utilized to generate strong SERS signals after being attracted by a magnet, as shown in Fig 1b.

2. Results and Discussion

The synthetic procedure of M AgNS is shown in Fig 1c. First, silica NPs were synthesized using the Stöber method [25] and analyzed by transmission electron microscopy (TEM), as shown in Fig 2a.

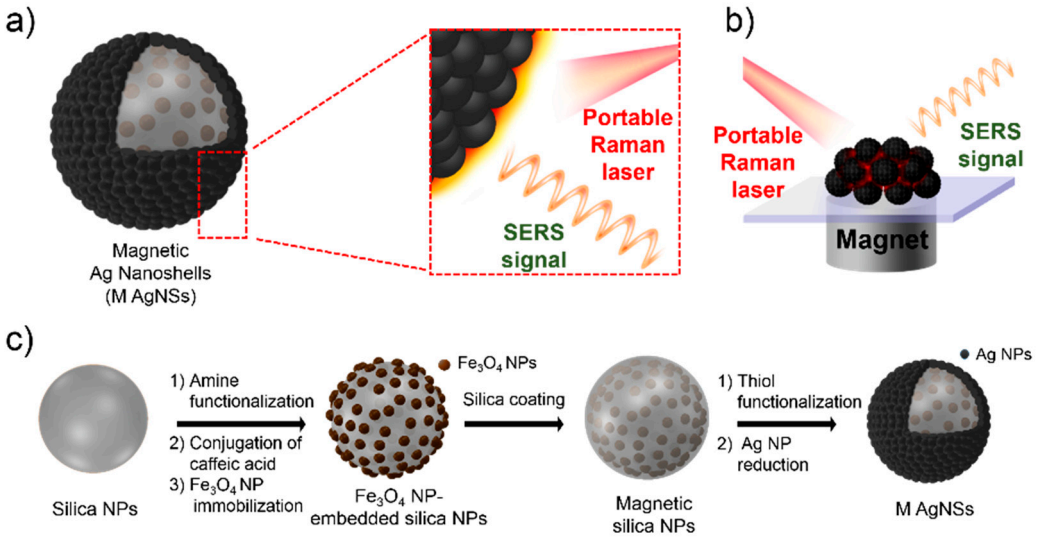

Figure 1. a) Structure of a magnetic silver nanoshell (M AgNS). The inset shows the enhanced SERS signal that arises from a bumpy M AgNS surface. b) Magnetic-induced aggregation procedure for sensitive target detection. c) Synthetic scheme for M AgNSs.

The silica NPs were spherical and monodispersed (250 ± 10 nm). Then, amine groups were introduced onto the surface of the silica NPs by reacting with 3-aminopropyltriethoxysilane (APTS). Caffeic acid was coupled to the amine groups on the silica NP's surface to introduce catechol groups. Then, oleate stabilized Fe_3O_4 NPs were treated with polyvinylpyrrolidone (PVP) to exchange the oleate ligand.

Peer-reviewed version available at Nanomaterials 2017, 7, , 146; doi:10.3390/nano7060146

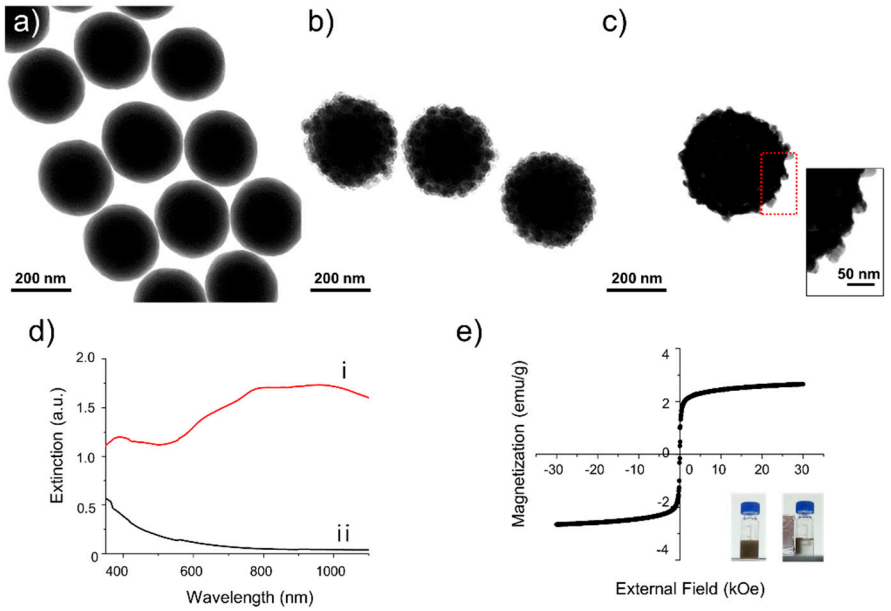

Figure 2. TEM images of a) silica NPs, b) magnetic silica NPs, and c) M AgNSs. d) UV-Vis absorption spectrum of i) M AgNSs and ii) magnetic silica NPs. e) Hysteresis loop of M AgNSs. The insets show photographic images of the M AgNSs before and after being attracted by a magnet for 5 min.

After treating with an excess of PVP with heat, the Fe_3O_4 NPs were well dispersed in the hydrophilic or amphiphilic solvent. Then, the PVP-stabilized Fe_3O_4 NPs were mixed with the catechol-functionalized silica NPs [26,27]. Additional silica encapsulation was conducted to prevent detaching of the Fe_3O_4 NPs from the silica NPs. Approximately 400 units of Fe_3O_4 NPs were assembled on each silica NP, and the thickness of the silica layer on the outer part of the magnetic silica NPs was approximately 10 nm, as shown in Fig 2b. Then, thiol groups were introduced onto the magnetic silica NPs by treating with 3-mercaptopropyltrimethoxysilane (MPTS). Silver ions were effectively reduced on the surface of the magnetic silica NPs because of the interaction between the thiol groups of MPTS and the silver ions, producing silver NPs and ultimately leading to the silver shell [28]. Octylamine and ethylene glycol have important roles in the nucleation and growth of silver NPs on the surface of the magnetic silica NPs [29]. The resulting NPs, M AgNSs, have a bumpy shell structure, as shown in Fig 2c.

The optical properties of the M AgNSs were characterized by UV-Vis spectroscopy (Fig 2d). From the extinction spectrum of the magnetic silica NPs, the unique absorption band in visible or IR region was not observed. However, the M AgNSs showed a broad extinction band in the NIR region (approximately 600 – 1100 nm), which is appropriate for NIR laser excitation during SERS analysis. The NIR absorption property correlates with the morphology of the bumpy silver surface of the M AgNSs, which determines the plasmonic property of the NPs [30].

We confirmed the magnetic property of the M AgNSs by analyzing the field dependent magnetization at 300 K. Because hundreds of Fe_3O_4 NPs are assembled, the M AgNSs exhibited a strong magnetic property, as shown in the magnetization curve (Fig 2e). The saturation magnetization of the M AgNSs was 2.7 emu/g, and there was no remanence magnetization when the external magnetic field was removed. The superparamagnetic property is essential for its analytical application because remanence magnetization in ferromagnetic material would cause NP's agglomeration [31]. We utilized Fe_3O_4 NPs (18 nm), which are small enough to maintain

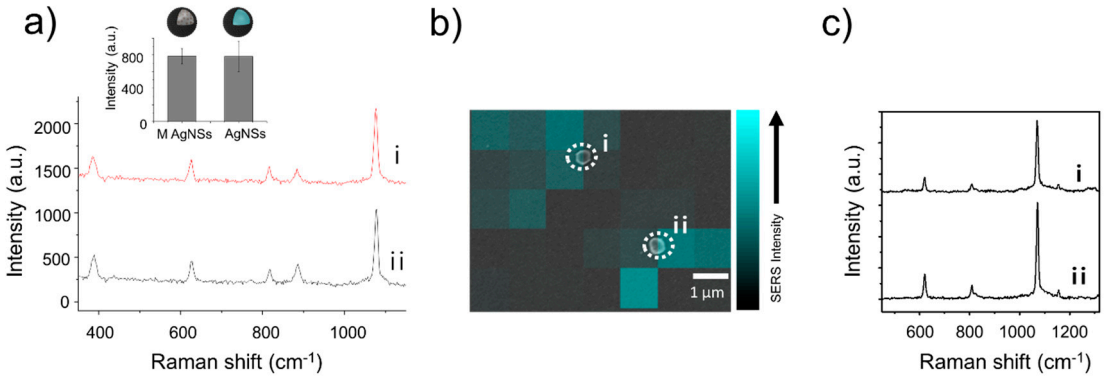

Figure 3. a) SERS spectra of 4-FBT on (i) M AgNSs and (ii) AgNSs. The inset shows the intensities of the 1075 cm^{-1} peak of 4-FBT. The spectra were obtained using a portable Raman system with a 785 nm laser at a power of 30 mW for 1 s. b) SERS intensity map of 4-FBT-treated M AgNSs. The corresponding SEM image was overlaid with the SERS map. (c) SERS spectra obtained from single M AgNS particles. Each spectrum (i, ii) corresponds to the single particles in SERS intensity map.

superparamagnetic properties, to provide superparamagnetic properties to the M AgNSs. The resulting M AgNSs were strongly attracted by a magnet within 5 min (Fig 2e, inset).

The SERS signal from the M AgNSs was obtained using a portable Raman system with 785-nm laser irradiation (Fig 3a). 4-Fluorobenzenethiol (4-FBT), a Raman reporter molecule, was incubated with the M AgNSs in ethanol. The thiol group of 4-FBT can interact strongly with the silver shell; thus, a SERS signal could be obtained from 4-FBT absorbed on the M AgNSs. The SERS intensity from the M AgNSs was compared to that from the AgNSs that have a similar structure as M AgNSs but without the Fe_3O_4 NPs. The AgNSs were prepared by forming a silver layer on silica NPs instead of magnetic silica NPs. The SERS intensities were determined by measuring the height of the 1075 cm-1 peak (the highest peak in the spectrum of 4-FBT) in the SERS spectrum; the difference between the SERS intensities of the M AgNSs and AgNSs was not significant. This result suggests that the existence of Fe_3O_4 NPs at the inner part of the M AgNSs did not significantly affect the intensity of the SERS signal. Furthermore, we collected the SERS signal from a single M AgNS particle. A drop of the M AgNS solution (0.5 mg/ml in ethanol) was placed on a patterned slide glass to measure the SERS signal. The SERS signal was collected using point-by-point mapping with a 1 μm step size using a 660 nm laser at a power of 2 mW with an exposure time of 1 s per point. Then, a scanning electron microscope (SEM) image was obtained in the same area in which the SERS mapping was performed. The location of each M AgNS particle was aligned exactly with the SERS map. As shown in Fig 3b-3c, the SERS signal intensity from the M AgNSs was strong enough to be detected at the single particle-level.

To evaluate the effectiveness of magnetic-induced aggregation, we investigated the SERS signal of the M AgNSs after being attracted by a magnet. The 4-FBT-treated M AgNSs were re-dispersed in water, and a drop of the solution (0.5 mg/ml) was placed on a glass slide. Then, we placed a magnet underneath the glass slide, as shown in Fig 1b. After 10 min, the M AgNSs were completely accumulated around the magnet. In contrast, when a drop of the AgNS solution was placed on a glass slide in the same manner, the magnet did not collect the AgNSs because they have no magnetic property. As shown in Fig 4a, the SERS intensity of the aggregated M AgNSs is 12 times stronger than that of the non-aggregated AgNSs, showing the strong enhancement of the SERS signal by magnetic-induced aggregation. Different concentrations of 4-FBT solutions were treated with M AgNSs to investigate the limit of detection (LOD) by this method. As shown in Fig 4b, the intensity of the SERS signal decreased as the concentration of 4-FBT decreased. And finally, the SERS signal of 4-FBT could be obtained at a concentration as low as 1 nM, which corresponds to 0.16 ppb.

Furthermore, we treated tetramethylthiuram disulfide (thiram) solution with M AgNSs to investigate its ability to detect a trace amount of the pesticide. A drop of the thiram-treated M AgNS

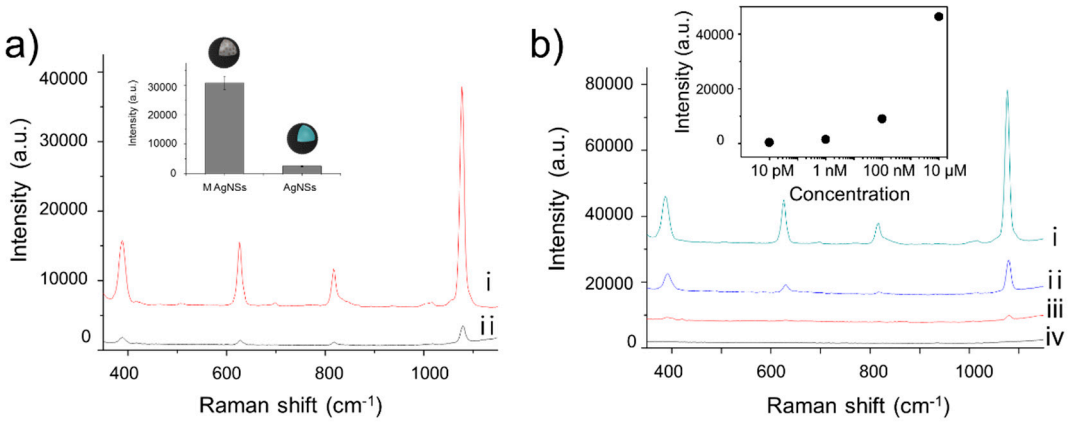

Figure 4. a) SERS spectra of 4-FBT on i) M AgNSs and ii) AgNSs after being attracted by a magnet. The inset shows the intensities for the 1075 cm^{-1} peak of 4-FBT. The spectra were obtained using a portable Raman system with a 785 nm laser at a power of 3 mW for 1 s. b) SERS spectra of 4-FBT on M AgNSs. The concentrations of 4-FBT were i) 10 μM, ii) 100 nM, iii) 1 nM, and iv) 10 pM. The inset shows the intensities of the 1075 cm^{-1} peak of 4-FBT. The spectra were obtained using a 785 nm laser at a power of 30 mW for 1 s.

solution was placed on a glass slide and attracted by a magnet for 10 min. The SERS signal from the thiram molecules on the M AgNSs could be obtained using a portable Raman system. The LOD for thiram was 10 μM, which corresponds to 3 ppm (Fig S1).

3. Materials and Methods

3.1. Materials

All reagents are used without further purification process. Oleate-stabilized Fe_3O_4 nanoparticles (NPs) was purchased from Ocean Nanotech. Absolute ethanol was purchased from Carlo Erba. Tetraethyl orthosilicate (TEOS), ammonium hydroxide (NH_4OH, 28 wt% in water), 3-aminopropyltriethoxysilane (APTS), caffeic acid, 3-mercaptopropyltrimethoxysilane (MPTS), silver nitrate ($AgNO_3$), ethylene glycol, polyvinylpyrrolidone (PVP, MW 10000 and 40000), octylamine, and 4-FBT (4-fluorobenzenethiol) were purchased from Sigma Aldrich. 2-(1H-Benzotriazole-1-yl)-1,1,3,3-tetramethyluronium hexafluoro- phosphate (HBTU) and hydroxybenzotriazole (HOBt) were purchased from Bead Tech. Tetramethylthiuram disulfide (thiram) was purchased from Alfa Aesar. Ethanol (95 %), N,N-dimethylformamide (DMF), methylene chloride (MC), diethyl ether, and N,N-diisopropylethylamine (DIEA) were purchased from Daejung Chemical.

3.2. Synthesis of magnetic silica NPs

Silica NPs were synthesized according to the well-known Stöber method. TEOS (1.6 ml) and NH_4OH (4 ml) were added to absolute ethanol (40 ml, 99.5 %) and stirred for 18 h at room temperature. The resulting silica NPs were centrifuged (7000 rpm, 15 min) and washed with ethanol several times. To introduce amine functional groups, silica NPs (40 mg) dispersed in ethanol (20 ml) were reacted with APTS (100 μl) and NH_4OH (100 μl) for 18 h. The reaction mixture was centrifuged (7000 rpm, 15 min) and washed with DMF several times. The resulting amine functionalized silica NPs (20 mg) were dispersed in DMF (5 ml), and reacted with caffeic acid (7.2 mg) and same equivalent of HBTU, HOBt, and DIEA for 3 h. The resulting catechol-functionalized silica NPs were centrifuged (7000 rpm, 15 min) and washed with DMF. Meanwhile, in order to stabilize Fe_3O_4 NPs with PVP (MW 10000), oleate-stabilized Fe_3O_4 NPs (2.5 mg dispersed in 100 μl chloroform) were poured into DMF/MC co-solvent (1:1 v/v, 5 ml) and PVP (120 mg) was added. The mixture was sonicated and

heated to 100 ℃ for 3 h, and cooled. The PVP-stabilized Fe_3O_4 NPs were slowly transferred into diethyl ether (10 ml). The solution was centrifuged (4500 rpm, 5 min) and re-dispersed in ethanol. The PVP-stabilized Fe_3O_4 NPs (0.08 mg/ml in 5 ml ethanol) and catechol-functionalized silica NPs (0.2 mg/ml in 5 ml DMF) were mixed and sonicated for 1 h. The mixture was centrifuged (6000 rpm, 10 min) and washed with ethanol. For silica coating, TEOS (50 μl) and NH_4OH (100 μl) were added to the Fe_3O_4 NPs-embedded silica NPs (dispersed in 5 ml ethanol) and reacted for 18 h. The resulting magnetic silica NPs were centrifuged (6000 rpm, 10 min) and washed several times with ethanol.

3.3. Synthesis of M AgNSs and AgNSs

To obtain thiolated magnetic silica NPs, MPTS (10 μl) and NH_4OH (50 μl) were added to the magnetic silica NPs suspension (1 mg/ml in ethanol). The mixture was shaken for 1 h at 50 °C. The resulting thiolated magnetic silica NPs were centrifuged (13000 rpm, 5 min) and washed several times with ethanol to remove excess reagent. Then, the thiolated magnetic silica NPs were dispersed in ethanol (100 μl). For the introduction of Ag shell, thiolated magnetic silica NPs (10 mg/ml in 50 μl ethanol) were added to PVP solution (MW 40000, 0.2 mg in 1 ml ethylene glycol), followed by mixing with ethylene glycol solution (1 ml) that contains $AgNO_3$. Final concentration of $AgNO_3$ was 7.3 mM. Then octylamine (4 μl) was poured quickly into the solution and the mixture was stirred for 1 h at 25 °C. The final product was centrifuged (13000 rpm, 5 min) and washed several times with ethanol. Meanwhile, AgNSs were prepared by using silica NPs solution (1 mg/ml in ethanol) instead of magnetic silica NPs solution, and the following process was identical to the synthesis of M AgNSs.

3.4. Characterization of NPs

Transmission electron microscopic (TEM) images were obtained by a LIBRA 120 (Carl Zeiss, Germany). UV/Vis extinction spectra were obtained with an Optigen 2120UV. Field-dependent magnetization was analysed with PPMS-14 (Quantum Design, USA). The SERS spectra were obtained with portable Raman system (i-Raman, B&W TEK). SERS mapping was proceeded with a micro-Raman system (LabRam 300, JY-Horiba). SEM images were obtained with SUPRA 55VP (Carl Zeiss, Germany).

3.5. Single particle SERS measurement

M AgNSs (0.5 mg) were added to 4-FBT solution (1 mM in ethanol) and reacted for 1 h. Then, the mixture was centrifuged (13000 rpm, 5 min) and washed several times with DI water. A drop (10 μl) of M AgNSs solution (0.5 mg/ml in 1 ml DI water) was put on a patterned slide glass. After obtaining point-by-point SERS mapping image with a 1-μm step size for 1s using a 660 nm laser line, the corresponding region was investigated by SEM image.

3.6. Magnetic-induced aggregation of M AgNSs

For obtaining SERS signal from 4-FBT, M AgNSs (0.5 mg) were dispersed in ethanol containing 4-FBT, and incubated for 1 h. The mixture was centrifuged (13000 rpm, 5 min) and washed several times with DI water. A drop (10 μl) of M AgNSs solution (0.5 mg/ml in 1 ml DI water) was transferred to a glass slide. Then a magnet was located underneath the glass slide, and M AgNSs were accumulated by the magnet for 10 minutes. For obtaining SERS signal from thiram, M AgNSs were dispersed in ethanol containing thiram, and reacted for 1 h. Then, a drop (2 μl) of M AgNSs solution (0.5 mg/ml in 1 ml ethanol) was transferred to a glass slide. After a magnet was located underneath the glass slide, the NPs were accumulated for 10 minutes.

4. Conclusions

We have fabricated M AgNSs, which has both magnetic and SERS properties for sensitive detection of chemicals. The M AgNSs contain hundreds of Fe_3O_4 NPs and have a bumpy silver shell. Thus, a strong SERS signal could be obtained from the absorbed target because of the bumpy structure and magnetic-induced aggregation. The sensitivity of this method was confirmed by obtaining the SERS signal from a trace amount of molecules in a solution with a portable Raman system. Furthermore, rapid accumulation of the M AgNSs caused by the strong magnetic response provides great advantages for on-site detection of contaminants. Based on the magnetic-SERS dual functionality, M AgNSs are expected to be utilized as a practical and effective nanoprobe for on-site and highly-sensitive detection of contaminants.

Supplementary Materials: The following are available online at www.mdpi.com/link, Figure S1: SERS spectra of i) thiram-treated M AgNSs and ii) non-treated M AgNSs after being accumulated by using a magnet.

Acknowledgments: This research was supported by the Pioneer Research Center Program through the National Research Foundation of Korea, funded by the Ministry of Science, ICT & Future Planning (Grant Number 2013-006163), and supported by the Bio & Medical Technology Development Program through the National Research Foundation (NRF) and funded by the Korean government (MSIP & MOHW) (2016-A423-0045).

Author Contributions: Cheolhwan Jeong, Hyung-Mo Kim, Bong-Hyun Jun, and Yoon-Sik Lee conceived the idea and designed the experiments. Cheolhwan Jeong, Hyung-Mo Kim, So Yeon Park, and Yuna Ha performed the experiments. Myeong Geun Cha, San Kyeong, Xuan-Hung Pahm, Eunil Hahm, and Dae Hong Jeong analyzed the data. Cheolhwan Jeong and Hyung-Mo Kim wrote the manuscript. Bong-Hyun Jun and Yoon-Sik Lee supervised the research.

Conflicts of Interest: The authors are declared no conflict of interest.

References

1. Schlücker, S. Sers microscopy: Nanoparticle probes and biomedical applications. *ChemPhysChem* **2009**, *10*, 1344-1354.
2. Amendola, V.; Scaramuzza, S.; Agnoli, S.; Polizzi, S.; Meneghetti, M. Strong dependence of surface plasmon resonance and surface enhanced raman scattering on the composition of au–fe nanoalloys. *Nanoscale* **2014**, *6*, 1423-1433.
3. Jaworska, A.; Jamieson, L.E.; Malek, K.; Campbell, C.J.; Choo, J.; Chlopicki, S.; Baranska, M. Sers-based monitoring of the intracellular ph in endothelial cells: The influence of the extracellular environment and tumour necrosis factor-α. *Analyst* **2015**, *140*, 2321-2329.
4. Dougan, J.A.; Faulds, K. Surface enhanced raman scattering for multiplexed detection. *Analyst* **2012**, *137*, 545-554.
5. Kim, H.-M.; Jeong, S.; Hahm, E.; Kim, J.; Cha, M.G.; Kim, K.-M.; Kang, H.; Kyeong, S.; Pham, X.-H.; Lee, Y.-S., *et al.* Large scale synthesis of surface-enhanced raman scattering nanoprobes with high reproducibility and long-term stability. *J. Ind. Eng. Chem.* **2016**, *33*, 22-27.
6. Tang, J.-j.; Sun, J.-f.; Lui, R.; Zhang, Z.-m.; Liu, J.-f.; Xie, J.-w. New surface-enhanced raman sensing chip designed for on-site detection of active ricin in complex matrices based on specific depurination. *ACS Appl. Mater. Interfaces* **2016**, *8*, 2449-2455.
7. Qi, M.; Huang, X.; Zhou, Y.; Zhang, L.; Jin, Y.; Peng, Y.; Jiang, H.; Du, S. Label-free surface-enhanced raman scattering strategy for rapid detection of penicilloic acid in milk products. *Food chem.* **2016**, *197*, 723-729.

8. Li, Y.-T.; Qu, L.-L.; Li, D.-W.; Song, Q.-X.; Fathi, F.; Long, Y.-T. Rapid and sensitive in-situ detection of polar antibiotics in water using a disposable ag–graphene sensor based on electrophoretic preconcentration and surface-enhanced raman spectroscopy. *Biosens. Bioelectron.* **2013**, *43*, 94-100.
9. Wei, W.Y.; White, I.M. A simple filter-based approach to surface enhanced raman spectroscopy for trace chemical detection. *Analyst* **2012**, *137*, 1168-1173.
10. Radziuk, D.; Moehwald, H. Prospects for plasmonic hot spots in single molecule sers towards the chemical imaging of live cells. *Phys. Chem. Chem. Phys.* **2015**, *17*, 21072-21093.
11. Weissleder, R. A clearer vision for in vivo imaging. *Nat. biotechnol.* **2001**, *19*, 316-316.
12. Kang, H.; Jeong, S.; Park, Y.; Yim, J.; Jun, B.H.; Kyeong, S.; Yang, J.K.; Kim, G.; Hong, S.; Lee, L.P. Near‐infrared sers nanoprobes with plasmonic au/ag hollow‐shell assemblies for in vivo multiplex detection. *Adv. Funct. Mater.* **2013**, *23*, 3719-3727.
13. Kang, H.; Yang, J.-K.; Noh, M.S.; Jo, A.; Jeong, S.; Lee, M.; Lee, S.; Chang, H.; Lee, H.; Jeon, S.-J. One-step synthesis of silver nanoshells with bumps for highly sensitive near-ir sers nanoprobes. *J. Mater. Chem. B* **2014**, *2*, 4415-4421.
14. Kyeong, S.; Jeong, C.; Kim, H.Y.; Kang, H.; Yang, J.-K.; Lee, D.S.; Jun, B.-H.; Lee, Y.-S. Fabrication of mono-dispersed silica-coated quantum dot-assembled magnetic nanoparticles. *RSC Adv.* **2015**, *5*, 32072-32077.
15. Yang, K.; Hu, Y.; Dong, N. A novel biosensor based on competitive sers immunoassay and magnetic separation for accurate and sensitive detection of chloramphenicol. *Biosens. Bioelectron.* **2016**, *80*, 373-377.
16. Shin, M.H.; Hong, W.; Sa, Y.; Chen, L.; Jung, Y.-J.; Wang, X.; Zhao, B.; Jung, Y.M. Multiple detection of proteins by sers-based immunoassay with core shell magnetic gold nanoparticles. *Vib. Spectrosc.* **2014**, *72*, 44-49.
17. Rho, W.-Y.; Kim, H.-M.; Kyeong, S.; Kang, Y.-L.; Kim, D.-H.; Kang, H.; Jeong, C.; Kim, D.-E.; Lee, Y.-S.; Jun, B.-H. Facile synthesis of monodispersed silica-coated magnetic nanoparticles. *J. Ind. Eng. Chem.* **2014**, *20*, 2646-2649.
18. Song, E.-Q.; Hu, J.; Wen, C.-Y.; Tian, Z.-Q.; Yu, X.; Zhang, Z.-L.; Shi, Y.-B.; Pang, D.-W. Fluorescent-magnetic-biotargeting multifunctional nanobioprobes for detecting and isolating multiple types of tumor cells. *ACS nano* **2011**, *5*, 761-770.
19. Lim, I.-I.S.; Njoki, P.N.; Park, H.-Y.; Wang, X.; Wang, L.; Mott, D.; Zhong, C.-J. Gold and magnetic oxide/gold core/shell nanoparticles as bio-functional nanoprobes. *Nanotechnology* **2008**, *19*, 305102.
20. Toma, S.H.; Santos, J.J.; Araki, K.; Toma, H.E. Pushing the surface-enhanced raman scattering analyses sensitivity by magnetic concentration: A simple non core–shell approach. *Anal. Chim. Acta.* **2015**, *855*, 70-75.
21. Kyeong, S.; Jeong, C.; Kang, H.; Cho, H.-J.; Park, S.-J.; Yang, J.-K.; Kim, S.; Kim, H.-M.; Jun, B.-H.; Lee, Y.-S. Double-layer magnetic nanoparticle-embedded silica particles for efficient bio-separation. *PloS one* **2015**, *10*, e0143727.
22. Yang, T.; Guo, X.; Wang, H.; Fu, S.; Yu, J.; Wen, Y.; Yang, H. Au dotted magnetic network nanostructure and its application for on‐site monitoring femtomolar level pesticide. *Small* **2014**, *10*, 1325-1331.
23. Gan, Z.; Zhao, A.; Zhang, M.; Wang, D.; Guo, H.; Tao, W.; Gao, Q.; Mao, R.; Liu, E. Fabrication and magnetic-induced aggregation of Fe_3O_4–noble metal composites for superior sers performances. *J. Nanopart. Res.* **2013**, *15*, 1954.

24. Wheeler, D.A.; Adams, S.A.; López‐Luke, T.; Torres‐Castro, A.; Zhang, J. Magnetic Fe_3O_4‐au core‐shell nanostructures for surface enhanced raman scattering. *Ann. Phys.* **2012**, *524*, 670-679.
25. Stöber, W.; Fink, A.; Bohn, E. Controlled growth of monodisperse silica spheres in the micron size range. *J. Colloid Interface Sci.* **1968**, *26*, 62-69.
26. Xu, C.; Xu, K.; Gu, H.; Zheng, R.; Liu, H.; Zhang, X.; Guo, Z.; Xu, B. Dopamine as a robust anchor to immobilize functional molecules on the iron oxide shell of magnetic nanoparticles. *J. Am. Chem. Soc.* **2004**, *126*, 9938-9939.
27. Chen, L.X.; Liu, T.; Thurnauer, M.C.; Csencsits, R.; Rajh, T. Fe_2O_3 nanoparticle structures investigated by x-ray absorption near-edge structure, surface modifications, and model calculations. *J. Phys. Chem. B* **2002**, *106*, 8539-8546.
28. Yang, J.-K.; Kang, H.; Lee, H.; Jo, A.; Jeong, S.; Jeon, S.-J.; Kim, H.-I.; Lee, H.-Y.; Jeong, D.H.; Kim, J.-H. Single-step and rapid growth of silver nanoshells as sers-active nanostructures for label-free detection of pesticides. *ACS Appl. Mater. Interfaces* **2014**, *6*, 12541-12549.
29. Kang, H.; Kang, T.; Kim, S.; Kim, J.-H.; Jun, B.-H.; Chae, J.; Park, J.; Jeong, D.-H.; Lee, Y.-S. Base effects on fabrication of silver nanoparticles embedded silica nanocomposite for surface-enhanced raman scattering (sers). *J. Nanosci. Nanotechnol.* **2011**, *11*, 579-583.
30. Jain, P.K.; Huang, X.; El-Sayed, I.H.; El-Sayed, M.A. Noble metals on the nanoscale: Optical and photothermal properties and some applications in imaging, sensing, biology, and medicine. *Acc. Chem. Res.* **2008**, *41*, 1578-1586.
31. Lu, A.H.; Salabas, E.e.L.; Schüth, F. Magnetic nanoparticles: Synthesis, protection, functionalization, and application. *Angew. Chem. Int. Ed.* **2007**, *46*, 1222-1244.